



IMAGE LICENSED BY INGRAM PUBLISHING

Amping Up the PA for 5G

Zoya Popovic

Signals designed for high-capacity communications result in high peak-to-average ratio (PAR) waveforms that the transmitter power amplifier (PA) must amplify with low distortion. With emerging fifth-generation (5G) wireless systems, carrier frequencies and signal bandwidths are expected to increase significantly from the current S- and C-band allocations. All these factors are

contributing to the increasingly challenging goals of maintaining transmitter PA efficiency for the following reasons:

- Efficiency is not constant over output power.
- Highly efficient PAs are usually nonlinear.
- RF load variations can adversely impact efficiency.

This article briefly reviews supply modulation to enhance the efficiency of several PA types, followed by

Zoya Popovic (zoya@colorado.edu) is with the University of Colorado, Boulder, United States.

Digital Object Identifier 10.1109/MMM.2017.2664018

Date of publication: 7 April 2017

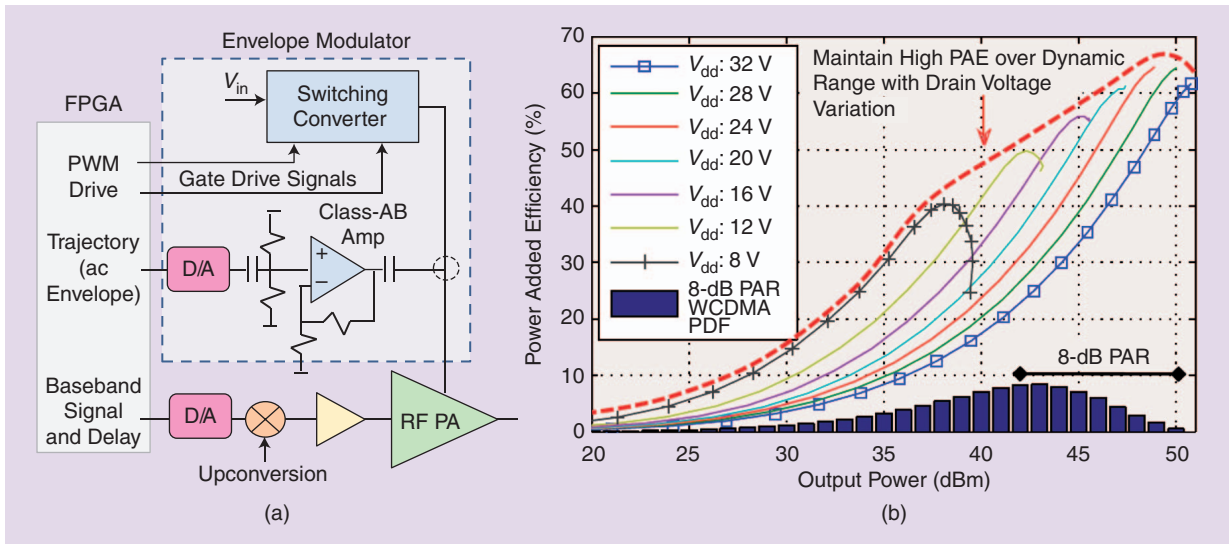


Figure 1. (a) An ET PA transmitter block diagram showing the digital baseband and control portion implemented in a field-programmable gate array (FPGA); the envelope modulator consists of a high-efficiency, slow-switching supply combined with a fast, less-efficient linear amplifier operating at the signal envelope bandwidth of tens to hundreds of megahertz, while the RF PA with driver operates at the carrier frequency in the gigahertz range. (b) Sample PAE curves for a GaN PA as a function of output power for various supply voltages showing the desired supply-voltage variations for high-to-average-efficiency operation. PWM: pulse-width modulation; D/A: digital to analog; WCDMA: Wideband Code-Division Multiple Access; PDF: probability density function.

a discussion of the main challenges and some predictions about where this technology might be headed in the future.

Supply modulation, or envelope tracking (ET), is included as an element in several commercially available handsets within the lower microwave frequency range (up to 2 GHz), as applied to subwatt power-level gallium arsenide (GaAs) PAs. This article extends the discussion to higher-frequency PAs implemented in gallium nitride (GaN). Specific examples of supply-modulated GaN transmitters with carrier frequencies in the 10-GHz range and signal bandwidths in the hundreds of megahertz range are provided, and challenges for further bandwidth increase are discussed.

Introduction and Background

The block diagram in Figure 1(a) reviews a basic ET PA transmitter, in which the power-supply voltage provided to the PA is dynamically varied in accordance with the time-varying envelope of the signal so that the PA is kept nearly always in compression, where its efficiency is high [1], [2]. Figure 1(b) shows example power-added efficiency (PAE) plotted as a function of PA output power for several supply voltages: if a dynamic supply can follow the peaks of the PAE curves as the signal envelope (and, therefore, output power) varies, this approach could result in a substantial increase in the average efficiency of the RF PA. However, overall system efficiency includes losses in both the PA and the dynamic power supply (envelope modulator) and is challenging to implement with

the high efficiency, high accuracy, and high slew rate required for broadband signal amplification.

Figure 1(a) shows a typical implementation of the envelope modulator with an efficient but slow switching-mode converter combined with a less-efficient but faster linear amplifier (see, e.g., [3]). In cellular applications, ET is commercially used in handsets and has been proposed for base stations as well. In 2013, the Qualcomm QFE 1110 tracker chip for handsets was advertised as the first released tracker and was soon included in the transmitter of a number of 3G/4G phones (e.g., the Amazon Fire).

A summary of earlier published contributions applying supply modulation or other methods is shown in Table 1, which highlights selected work from [3]–[25]. The different PA types indicated in Table 1 (polar, wide-band ET (WBET), hybrid envelope elimination and restoration (HEER), linear amplification using nonlinear components (LINC), and supply modulated (SM)) are variations of supply modulation and are discussed in detail in [26]. The demonstrations are mostly at or below S-band and show some high composite PAEs (CPAEs), even above 60% for signals with in-phase/quadrature (I/Q) bandwidths below 5 MHz.

In early X-band work [7], GaAs metal–semiconductor field-effect transistor X-band PAs were characterized statically. More recently, ET with higher signal bandwidth has been demonstrated; e.g., [27] reported 100-MHz I/Q bandwidth for an X-band PA with a 70% efficient envelope modulator.

While Figure 1 illustrates the standard ET approach, Figure 2 describes several supply-modulated transmitter architectures at the highest level. The three architectures commonly proposed for increasing efficiency are the Doherty amplifier, outphasing amplifier, and ET amplifier. The latter necessarily includes supply modulation, while Doherty and outphasing amplifiers can be improved further by adding a variable supply. PA1 and PA2 are at the same carrier frequency in both the Doherty and outphasing approaches. Although both are characterized by load modulation, the output combiners are different, and the two PAs are the same only in the outphasing case.

Important Considerations for Supply-Modulated Transmitter Designs

In all approaches that include supply modulation, whether ET, Doherty, or outphasing, there is an increase in complexity and part count, as well as the need for additional linearization. For any of the architectures to be practical, the performance gain must be significant enough to warrant the increased complexity and cost. This subject is discussed in, e.g., [21], where two trajectories are compared for the same experimental GaN PA and a custom-designed supply modulator. One case described the simplest drive modulation with constant supply (in this case, 32 V for a 0.25- μm GaN process) and a trajectory resembling curve G in Figure 3 with a peak reaching 32 V. The results are summarized in Table 2. Note that the supply-modulated trajectory results in a measured composite average transmitter PAE of 52.5%, with 8-W average output power for a 7-dB PAR signal having a 23-MHz supply-modulator bandwidth. The linearity is met for Wideband Code-Division Multiple Access (WCDMA) downlink signals, with an error-vector magnitude (EVM) below 1%. To meet linearity in this case, the PA average drain efficiency was 75.9%, compared to 30% for the constant drain-voltage case.

An interesting conclusion can be drawn from the results in Table 2 by observing the dissipated heat for the two trajectories. When the ET trajectory is compared to a constant-supply case for this efficient PA, calculations show that, operating from a battery, the supply-modulated transmitter would last 75% longer and in a fixed installation consume 43% less power. PA dissipation is reduced from 19.8 W to only 2.7 W, also reducing the cooling requirements. In the supply-modulated transmitter, 61% less heat is produced; more

TABLE 1. An overview of existing techniques with supply modulation.

Reference	Type	f (GHz)	Bandwidth (MHz)	PAR (dB)	P_{out} (W)	CPAE
[3], 1999	ET	0.9	10	6	5	35%
[7], 2004	Polar	10	static	5	0.12	22-65%
[9], 2006	WBET	2.14	3.84	7.67	37.2	50.7%
[10], 2008	Polar	0.9	27.6	9.6	1	41%
[14], 2009	HEER	2.655	5	8.2	16	40%
[15], 2009	LINC	2.14	3.84	9.6	90	50.5%
[16], 2009	ET	2.14	3.84	7.7	42	58%
[17], 2010	Doherty	2.14	3.84	8	10	50.9%
[19], 2011	ET	2.14	3.84	6.6	38.2	60.9%
[20], 2011	LINC	1.95	5	7.5	19	51.6%
[21], 2012	SM	2.14	23	7	35	52.5%
[22], 2012	ET	2.14	20	6.5	40.6	43.4%
[23], 2013	LINC	2.3	3.84	9.6	19	43.5%
[25], 2014	SM	10	18	7.1	5	62.6%

importantly, the transistor in the PA operates with 86% less heat, implying that the microwave transistors can be operated at a higher voltage with fewer thermally-introduced memory effects. The power dissipation is not only reduced but also divided between the PA and the supply modulator, further reducing heat-sinking requirements and thermal-device stress.

Supply-modulated PA systems are, in general, more complicated than traditional PAs. There are a number of challenges in implementing supply modulation in a PA, starting with high-efficiency PA design and including efficient supply design, linearization,

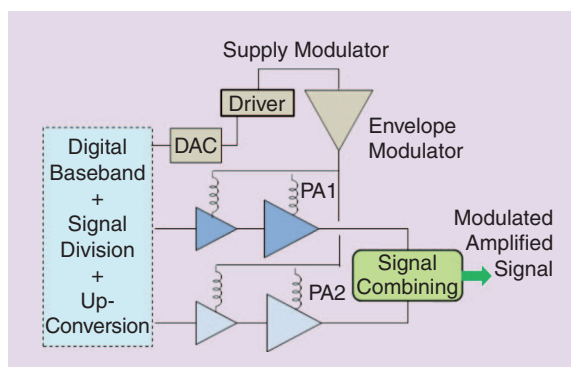


Figure 2. A general block diagram of transmitter architectures that improve efficiency for high PAR signals. PA1 and PA2 are at the same carrier frequency in both the Doherty and outphasing approaches. Although both are characterized by load modulation, the output combiners are different. PA1 and PA2 are the same only in the outphasing case. In ET, the output combining occurs in the PA. DAC: digital-to-analog converter.

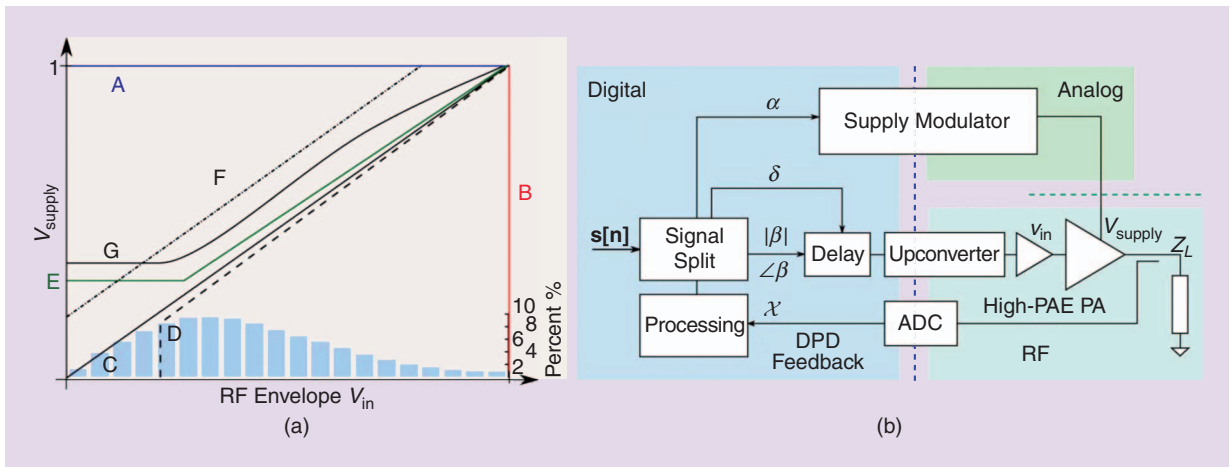


Figure 3. (a) Various trajectories that have been implemented in ET systems and (b) a block diagram of an ET system that would allow various trajectories and linearization [21]. The block “signal split” performs the trajectory operation in the digital baseband. ADC: analog-to-digital converter; DPD: digital predistortion.

and transmitter integration. One of the main difficulties is related to signal bandwidth. In various types of ET transmitters, the supply generally tracks the signal envelope continuously, which can be many times the bandwidth of the I/Q signal components. For the simple example of an LTE signal, the I/Q and envelope power spectral density of a four-tone signal and an LTE signal are shown in Figure 4, pointing to the dramatic increase in bandwidth that the envelope modulator needs to follow. Complex modulation signals with amplitude passing through zero will have sharp amplitude nulls in the time domain, increasing the bandwidth requirements.

TABLE 2. A performance comparison for constant supply and efficiency-optimized dynamic supply of a GaN PA with a 5-MHz 7-dB PAR signal [21]. The transistor dissipation is dramatically reduced, allowing colder operation in addition to power savings. The transistor operates with 86% less heat with ET [21].

5-MHz WCDMA, PAR =7 dB	Constant Supply	Optimized Trajectory
Peak/average P_{out}	40 W/8 W	40 W/8 W
Supply-modulator efficiency	–	70%
PA efficiency (2.14-GHz GaN)	30%	75.9%
ACPR @ 5/10 MHz	–57/–58.3 dB	–55.7/–57.8 dB
Transmitter CPAE	30%	52.5%
Transmitter supply power	28.3 W	16.2 W
PA heat dissipation	19.8 W	2.7 W

For signals where a supply has the required bandwidth, it is still not advantageous to modulate the entire envelope through the supply, resulting in a trajectory of V_{supply} versus RF envelope (V_{in} or V_{out}). This is because a supply is typically more efficient for higher voltage levels and a limited voltage swing; at low power levels, the efficiency is not as important, and drive modulation is a better choice. The supply range depends on the type of signal, as well as on the type of PA. Figure 3(a) illustrates several possible input trajectories that have been reported in the literature, defined as the generally nonlinear dependence $V_{supply}(V_{in})$, including the traditional linear PA with constant V_{supply} (line A), envelope elimination and restoration with constant and full supply modulation (B), ET (C), partial drain modulation (D), partial supply modulation (E), offset supply for minimum drive (F), and following the best path for a given parameter (e.g., gain, linearity, or efficiency) (G). The envelope voltage probability density function (PDF) of a WCDMA signal preprocessed for a 7-dB PAR is also shown for comparison.

The envelope modulator needs to be efficient, while at the same time supporting increasingly large signal bandwidths, which implies large slew rates. For pulse-width modulation (PWM)-controlled switched-mode power supplies, this further implies even higher switching frequencies [28], resulting fundamentally in a drop in efficiency. Further, the envelope modulator load is the PA under large-signal operation, which is typically not well characterized with the nonlinear model in the low-frequency (envelope-bandwidth) range. When the signal bandwidth is high, this complex impedance can vary considerably from dc to some hundreds of megahertz [29], a variation that must be taken into account in the design of the dynamic supply.

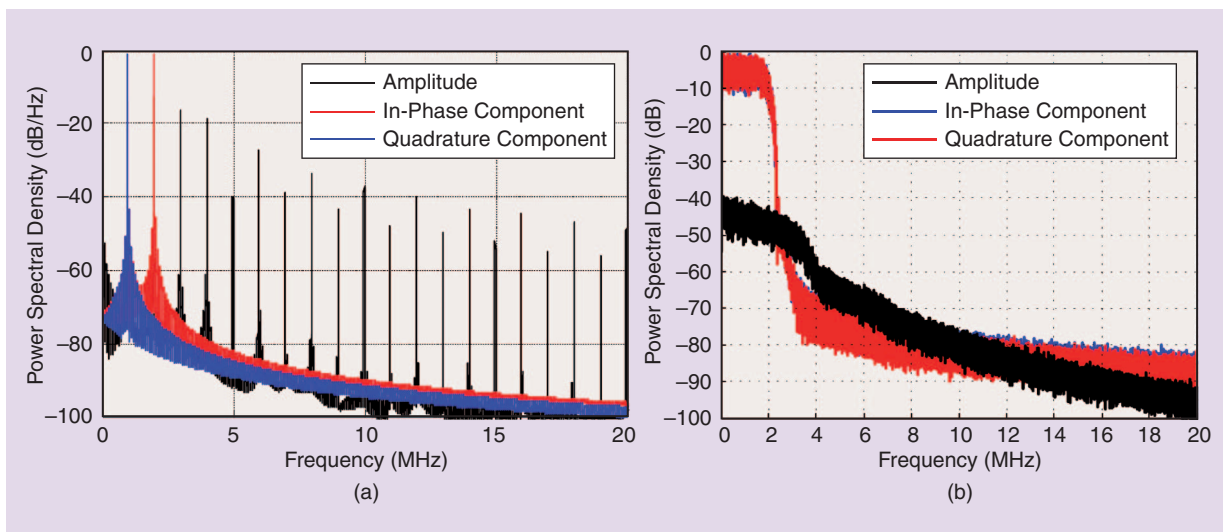


Figure 4. (a) The I (red), Q (blue), and envelope (black) power spectral densities for a four-tone signal and (b) an LTE signal, showing the expansion of bandwidth that the supply has to track. While the I and Q are well within a 5-MHz bandwidth, the amplitude bandwidth has frequency components well beyond 20 MHz of the signal [21].

The PA design is also nontraditional: the PA cannot be generally designed to function in any specific mode of operation (e.g. class-F or class-E) because the device nonlinear impedances at the fundamental and harmonics depend on the supply voltage. Therefore, the active device nonlinear model has to be fit to a range of supply voltages. The PA drain bias line must be a low-pass filter that passes the entire envelope bandwidth (sometimes several hundreds of megahertz), which implies eliminating bypass capacitors. This can, in turn, affect PA stability and be difficult to analyze because the dynamic supply impedance across the entire band where the device has gain might not be known. When integrating the supply and the PA, the interconnect is often a special type of filter designed to meet the envelope bandwidth requirements and supply-PA impedance requirements. Integration of the entire transmitter can result in coupling between signals that are of very different time scales, e.g., the switching of the dynamic supply can introduce noise in the output. Shielding and layout, as well as miniaturization, become important.

Supply modulation (ET) is inherently nonlinear, and various forms of distortion exist in a supply-modulated transmitter. The carrier-frequency amplifier introduces nonlinear, time-invariable amplitude-to-amplitude modulation and amplitude-to-phase modulation, which can be corrected by a lookup table. The supply modulator generally introduces time-variable linear distortion, which can be corrected by digital equalization. Additionally, there are nonlinear memory effects, which depend on the device technology and bias-line design. It is wise to first understand and then separately correct the different distortions to avoid an overly complicated digital predistortion algorithm.

One of the nonlinearities unique to a supply-modulated transmitter is time misalignment between the envelope and drive-fed signals. The RF waveform is input at the gate (for a field-effect transistor device), while the supply waveform is input through the drain bias line, and these waveforms need to be properly time aligned. For example, for a 5-MHz WCDMA signal, the alignment needs to be within about 2% of the inverse signal bandwidth, or 4 ns. The delay can be determined by minimizing the adjacent-channel power ratio (ACPR), for example, or using specific signals such as Gaussian chirps to quickly determine the required delay. Additionally, modern systems include closed-loop feedback to adjust the timing. This monitoring system feeds back a replica of the PA output, downconverts and digitizes it, and compares the result with the desired signal. The distortion can be reduced digitally using digital predistortion, which is already used for linearization in many nonsupply-modulated transmitters, such as with Doherty PAs in base stations. The power cost of the auxiliary receiver for signal feedback is usually negligible compared to the gains in efficiency for the whole system.

Simulation of an entire ET transmitter is difficult, especially for broadband signals and when the PWM of the switching dc-dc converter is included. The convergence difficulty of envelope-transient simulations [30] is a result of the existence of multiple time constants and the need to combine harmonic balance, full-wave field analysis, and system-level analysis in one simulation. The efficiency measurements, in both simulation and hardware, include supply-modulator and PA efficiencies over time. The instantaneous as well as average efficiencies are relevant, and the latter depends on the signal statistics.

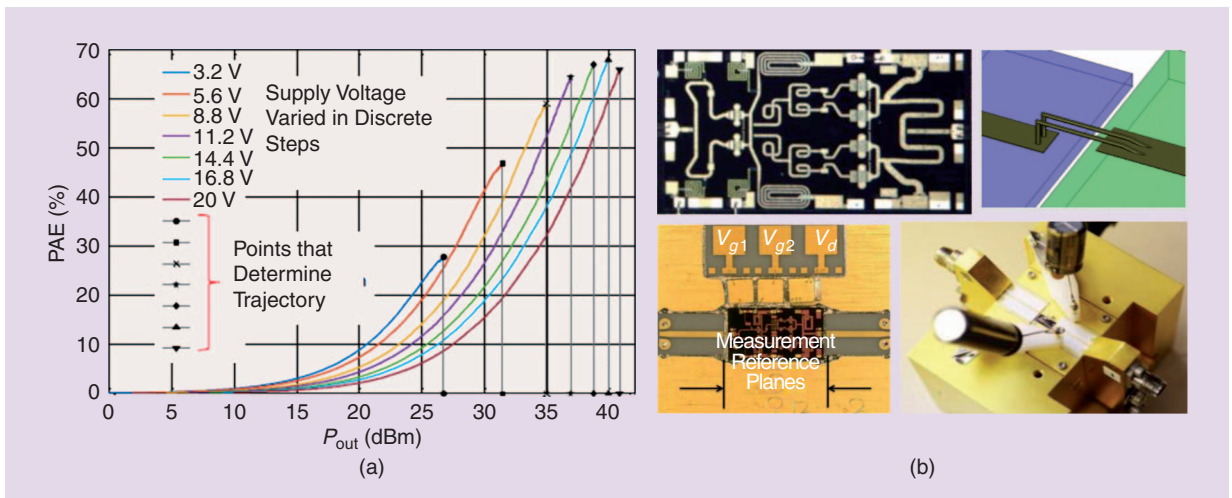


Figure 5. (a) The measured efficiency versus output power for several supply voltages of an X-band MMIC PA, 3.8 mm × 2.3 mm, fabricated in the GaN-on-SiC 150-nm Qorvo process. (b) The MMIC is mounted on a carrier and bonded to alumina 50-Ω lines. The bond wires are simulated in HFSS, and the reactance is included in the design of the MMIC.

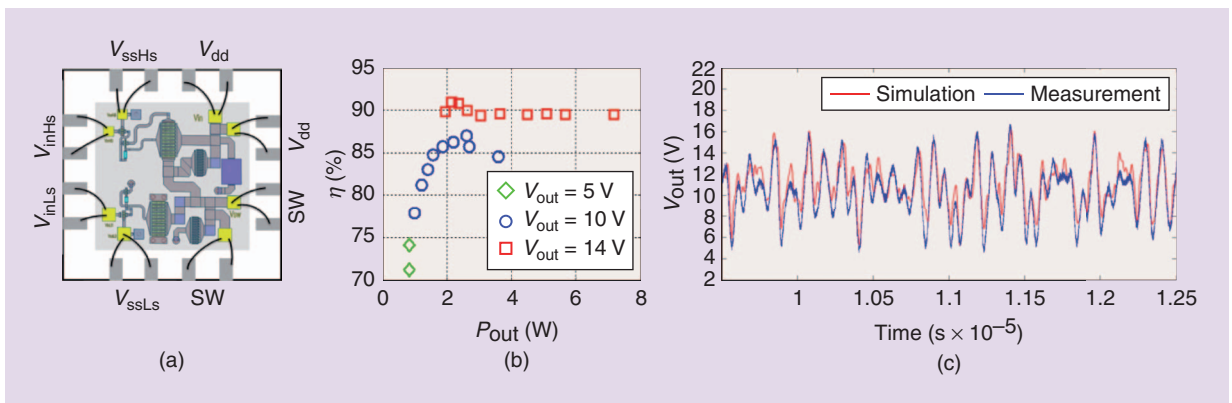


Figure 6. (a) The layout of the Buck converter MMIC packaged in a QFN package. (b) The measured efficiency at 100-MHz switching and (c) the measured and simulated tracking of a 20-MHz LTE signal.

GaN Monolithic Microwave Integrated Circuit PAs and Modulators for Dynamic-Supply Transmitters

The PAs for supply modulation presented in this article are designed in the Qorvo (TriQuint) 150-nm GaN-on-silicon carbide (SiC) process and are detailed in [24] and [25]. The PAs are designed with supply modulation in mind, where PAE, P_{out} , and gain are traded over a range of supply voltages. The simulated and measured static performance for a two-stage, 10-W PA is shown in Figure 5, where the measured data are obtained with the die bond-wired to fixture-alumina 50-Ω lines. The PA uses four $10 \times 90\text{-}\mu\text{m}$ devices in the output stage and has 20 dB of saturated gain. The simulations are performed with an Angelov-based model and include the bond-wire inductance to the outside alumina microstrip lines.

If the supply can be modulated at the envelope bandwidth and with high slew rates, the peak of the efficiency curves in Figure 5 (shown with dots) can be

tracked. For the PA shown in Figure 5, one can determine a “trajectory,” i.e., a prescribed function between the supply voltage and input signal envelope, to maximize efficiency, gain linearity, or power or with some tradeoff in mind: this is what the envelope modulator needs to follow. For signals with moderate bandwidths (a few tens of megahertz), this can be accomplished with continuous tracking using the architecture shown in Figure 1(a); if a very fast and efficient dc–dc converter is available, the fast linear amplifier is not needed. For signals with larger bandwidths, very fast supplies will have reduced efficiency, and a tradeoff can be made where average tracking is performed, e.g., [31], [32], using either a continuously varying dynamic supply or one with discrete multiple power levels.

A Buck switching converter modulator designed in the same 150-nm GaN process as the PA is shown in Figure 6, along with its measured efficiency when switching at 100 MHz [28], [33]. The circuit is measured in a standard quad flat no-lead (QFN) package, and

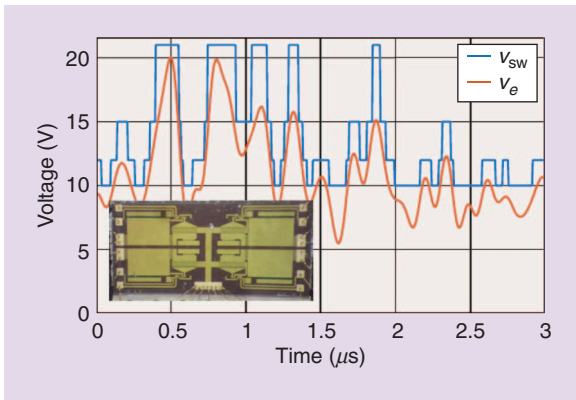


Figure 7. The output voltage of the four-discrete-level converter optimized for a 10-MHz LTE envelope signal and (inset) a photo of the GaN die. This converter achieves 97.3% power-stage efficiency.

the efficiency includes package losses and parasitics. To track the envelope of a 20-MHz LTE signal, a field-programmable gate array produces PWM sequences that provide the low-side and high-side signals.

Simulations in ADS Ptolemy with microwave non-linear models for the switching devices result in good agreement with the measurements, as shown in Figure 6(c). The root mean square error between the ideal envelope and the measured and simulated one is 4.5%. Such fast, efficient dc-dc converters implemented in a depletion-mode-only field-effect transistor process can also be combined in a multiphase converter topology for increased bandwidth tracking without reducing efficiency. Several such dc-dc converters are reported in [33] and [34].

For multilevel discrete tracking, two monolithic microwave integrated circuit (MMIC) multilevel supplies have been demonstrated: a four-level supply [35] and an eight-level, three-bit supply [36] with an architecture as described in [37]. Figure 7 shows tracking for the four-level MMIC, which achieves greater than 97.3% power-stage efficiency at 3.5-W average output power level for a 10-MHz LTE envelope signal.

Figure 8 shows the results for the eight-level MMIC supply when tracking an amplitude-modulated radar pulse with a 10-GHz carrier. Amplitude modulation is introduced to confine spectral content, and the ET makes it possible to maintain efficiency in this case, resulting from the high efficiency of both the PA (Figure 5) and the dynamic supply. The combined resulting efficiency is 44%, with a supply efficiency of 84% and PA efficiency of 52.4% averaged over the pulse duration with a 3.3-W power per pulse. Digital pre-distortion described in [36] and [37] results in a -52-dB first sidelobe level, compared to the -58-dB ideal case. For comparison, a rectangular pulse with the same frequency chirp has a -13-dB sidelobe level with a combined efficiency of 50%. The eight-level MMIC integrated with the PA MMIC was also characterized

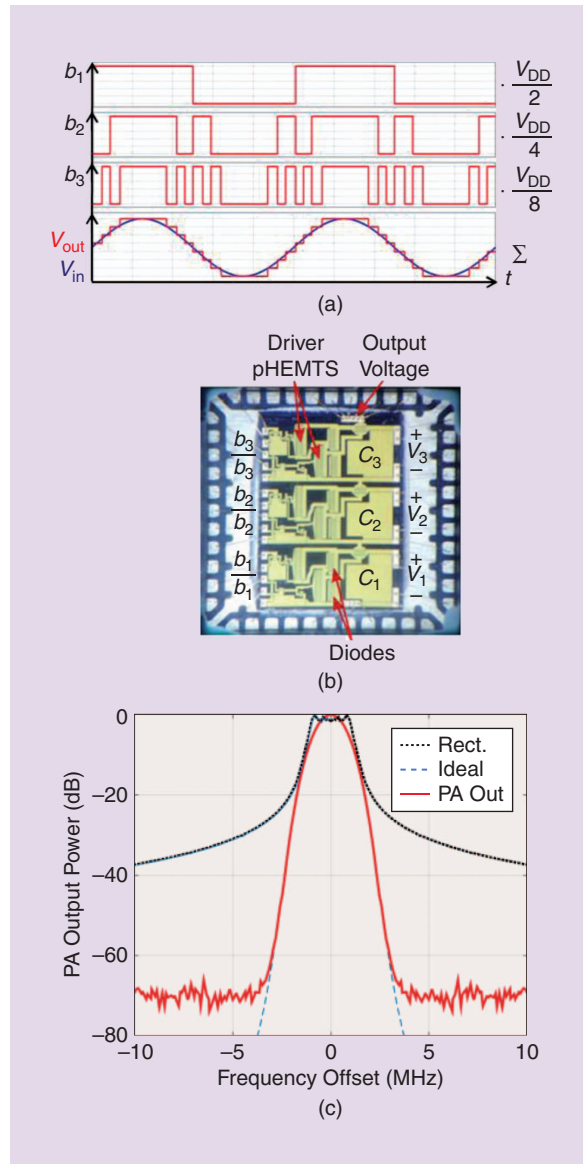


Figure 8. (a) The discrete tracking for (b) the eight-level GaN MMIC supply is illustrated with the sine wave example. (c) The measured spectrum is obtained at the output of the PA for an FM radar pulse with a Blackman-amplitude-modulated envelope, compared to a rectangular pulse. The spectral confinement is dramatically improved, while maintaining a total efficiency >44% at 10 GHz. pHEMT: pseudomorphic high-electron-mobility transistor.

with a 20-MHz LTE signal as well as with a Chireix PA MMIC [38].

Broadband Signal Tracking

Figure 9 shows the simulated total efficiency (ADS Ptolemy) of the PA from Figure 5 with the Buck converter tracker from Figure 6 for a 20-MHz LTE signal with a PAR = 7 dB. Compared to the constant-supply case at 20 V for an average power of 34 dBm, the time-average PAE improves from 26% to 48%, a 22-point improvement. In Figure 9, the instantaneous PAE and

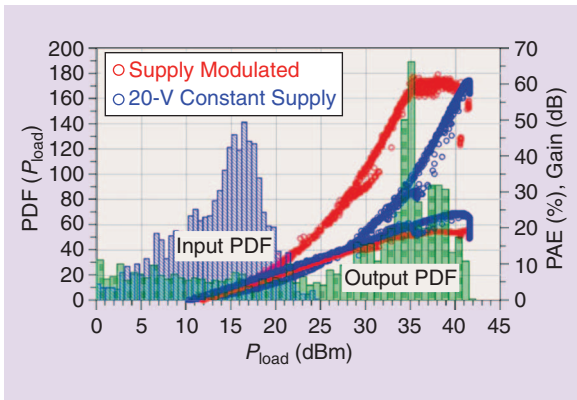


Figure 9. The simulated instantaneous PAE and saturated gain of the MMIC PA under supply modulation for an LTE signal, compared to the constant 20-V supply case. The input and output PDF of the LTE signal are plotted to show the PAE improvement against signal statistics. Both stages of the two-stage power-combined PA are modulated simultaneously in this case.

saturated gain are plotted together with the input and output PDF of the LTE signal. This efficiency improvement, however, significantly degrades as the signal bandwidth increases. For higher-bandwidth signals expected in the near future, an ultrahigh-frequency (UHF) amplifier can assist the Buck converter by amplifying higher-frequency signals efficiently. An example UHF cascode PA integrated in the same GaN process exhibits over 80% PAE with high gain above 120 MHz and over 60% up to 400 MHz [39]. This amplifier integrated with the switcher from Figure 6 can track a 130-MHz waveform, as demonstrated by the measurement in Figure 10.

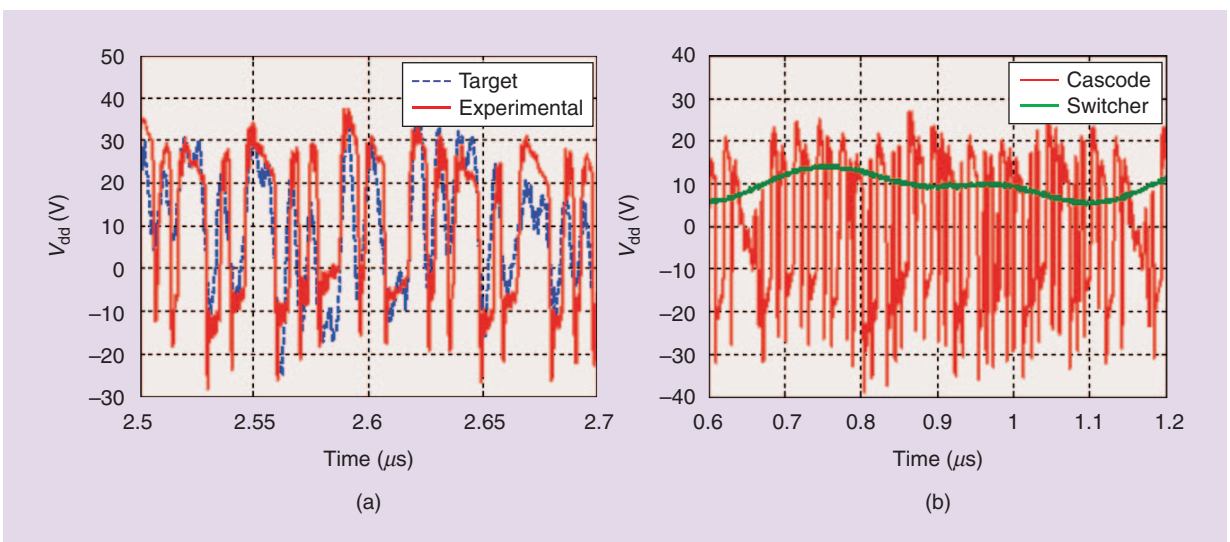


Figure 10. The measured results from the integration of the MMIC in Figure 6 with a cascode GaN MMIC PA from [39], (a) tracking for a 130-MHz orthogonal frequency-division multiplexing signal, where (b) the switcher covers dc–5 MHz and the cascode covers 5–130 MHz (ac-coupled for test purposes). The output power is 7.14 W with a total efficiency of 74.9%. The switcher output is 1.97 W at an average efficiency of 85.7%, while the cascode provides 5.17 W with an efficiency of 72.4%.

For the case of the eight-level supply, Figure 11 shows the output spectrum and time-domain envelope waveform measured for a 20-MHz LTE signal with PAR = 11.4 dB (digital predistortion applied). The total efficiency (PA combined with supply) at 10 GHz is 32%, with an average output power of 0.85 W, a measured EVM = 5.2%, and adjacent-channel leakage ratio = 33 dB. The fixed-supply efficiency is only 11% in this case, so we again see a 21-point improvement [36].

Because all necessary parts of an integrated broadband, X-band, supply-modulated PA have been demonstrated separately, the next step is full integration. A GaN MMIC that integrates a 10-GHz 10-W PA, a Buck converter with included drive circuitry, and a UHF cascode PA is shown in Figure 12, packaged with connectors for all the input and control signals included. The only off-chip component is a filter that determines the bandwidth division between the Buck and cascode circuits [40].

As commercial wireless communications evolve from 4G to 5G, the signal bandwidths are continually increasing. In carrier aggregation, where signals from more than one spectral band are transmitted simultaneously, a net large PAR results even for constant envelope signals. Some 5G systems are being allocated bands up into the millimeter-wave range (6–30 and 30–100 GHz) with envisioned signal bandwidths from 200 MHz to 2 GHz. This is also relevant to existing satellite multicarrier signals, with PARs in the 13-dB range and signal bandwidths well over 200 MHz. As an illustration of a possible approach to this problem, Figure 13 shows the envelope for a 250-MHz band-limited noise signal and its reduced bandwidth versions that can be accommodated with four-level tracking, which would result in a 20-point improvement in efficiency for a class-AB PA over direct drive modulation.

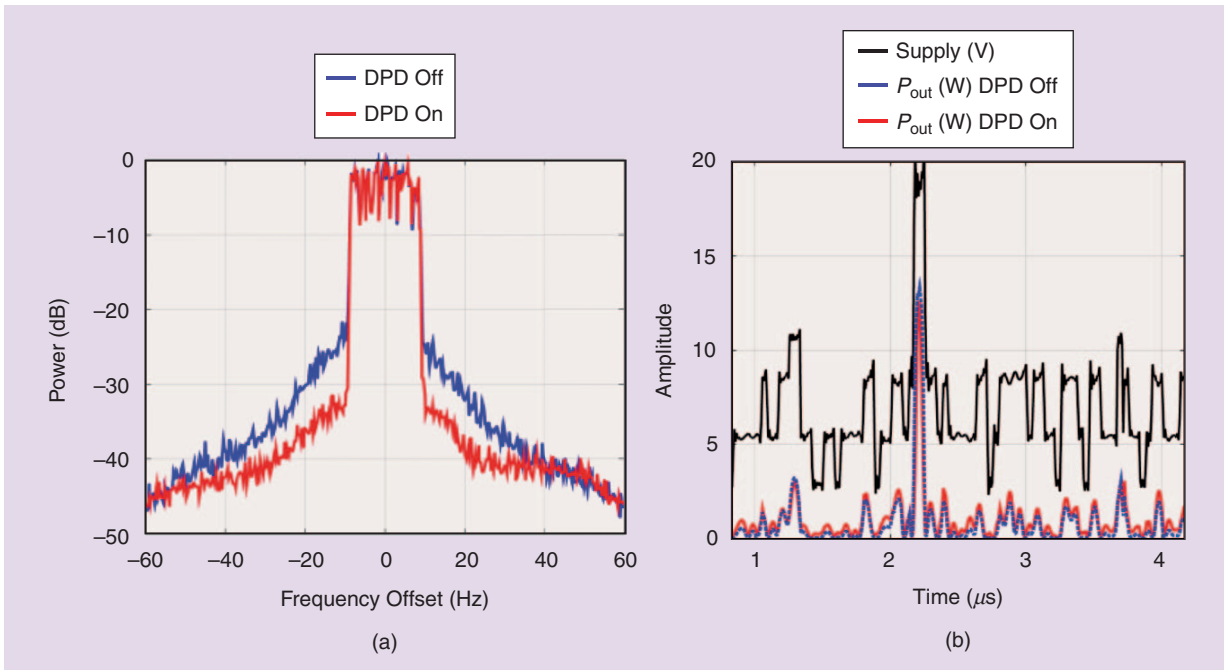


Figure 11. The (a) measured spectrum and (b) time-domain envelope waveforms for a 20-MHz LTE signal tracked by the eight-level supply [36] with 32% total PA and supply efficiency.

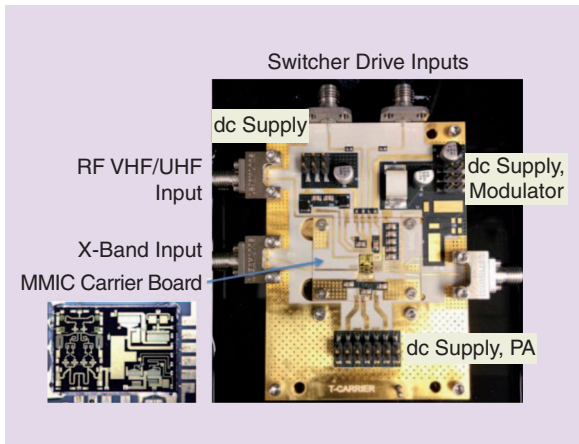


Figure 12. An integrated 10-GHz PA, Buck 100-MHz switching power supply, and UHF cascode PA packaged in a complete 5×6 -cm circuit, designed to efficiently track a signal with >300 MHz envelope bandwidth.

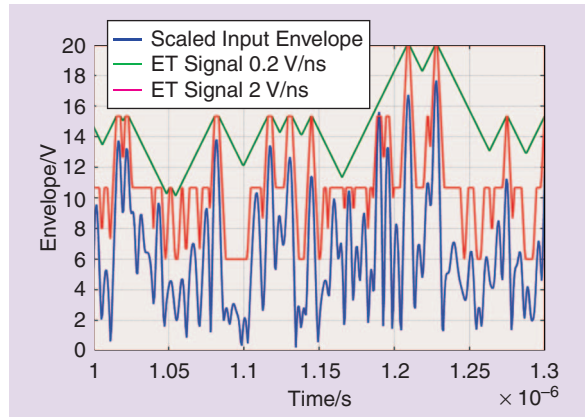


Figure 13. The simulated envelope for a 250-MHz band-limited noise signal and its reduced bandwidth versions that can be accommodated with four-level tracking. This would result in a 20-point improvement in efficiency for a class-AB PA over direct-drive modulation with constant-supply voltage.

Supply Modulation for Improving Efficiency of Doherty and Outphasing PAs

Supply modulation can be used to further improve the efficiency of load-modulated PA architectures, such as the Doherty and outphasing amplifiers. In a Doherty PA, supply modulation has been used for modulating the carrier (main) amplifier to increase the efficiency at higher backoff power levels [17], as shown in Figure 14. The efficiency versus backoff is sketched as well, showing possible improvements when only the main and both carrier and peaking amplifiers are tracked. A Doherty X-band GaN MMIC PA is characterized with supply modulation [41]. The measured output power of the chip,

shown in Figure 15, is greater than 36 dBm at peak PAE of 47% at 10 GHz. Gain flatness of ± 0.1 dB around 9.2 dB is obtained at up to 25-dBm input power. The PAE at 6- and 10-dB backoff is 41% and 31%, respectively. For a 10-Mb/s offset quadrature phase-shift keying signal, the ACPR (10 MHz) is >30 dBc at maximum output power and >33 dBc at 10-dB backoff, with no linearization.

In Chireix outphasing, a nonisolated combiner enables and dictates load modulation, maintaining high efficiency operation. In LINC outphasing, an isolated combiner preserves linear amplification at the cost of poor efficiency roll off with output power. One shortcoming of constant-supply outphasing PAs is the relatively large required

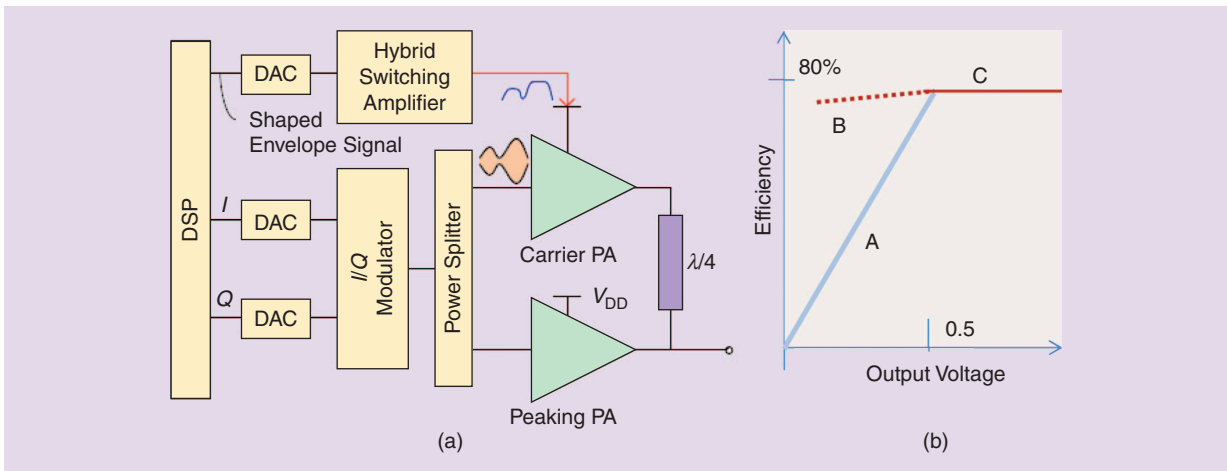


Figure 14. (a) An illustration of efficiency in Doherty PAs with only the carrier PA modulated: i.e., the dashed line B in (b) [17]. The efficiency can be further improved by modulating the peaking amplifier. DSP: digital signal processor.

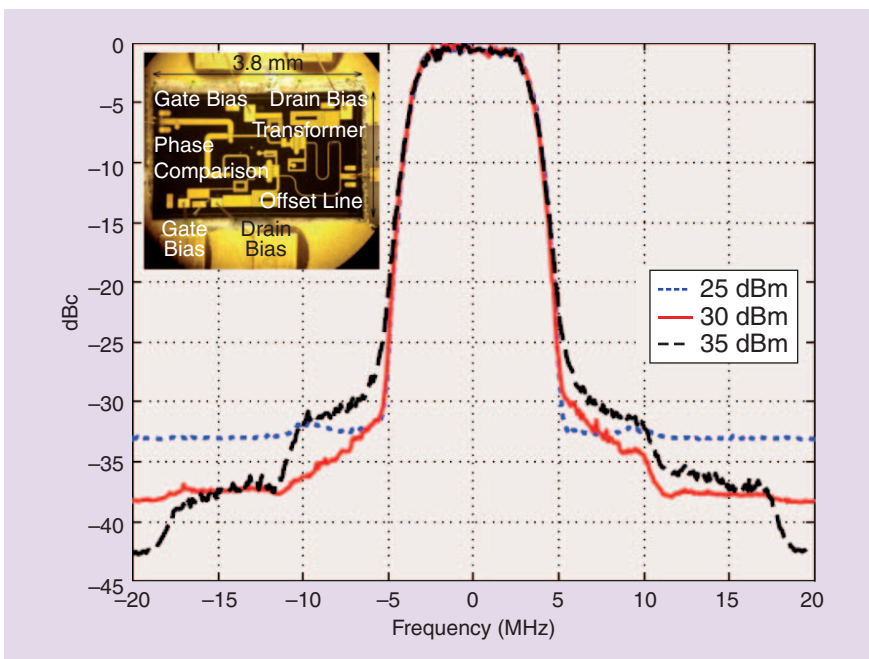


Figure 15. The measured linearity up to 10-dB backoff with no digital predistortion of a 10-GHz Doherty MMIC PA (shown in the inset).

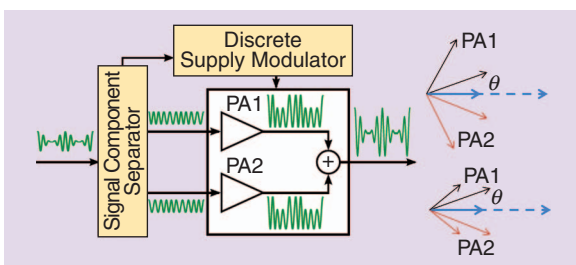


Figure 16. An outphasing PA with discrete multilevel supply voltage, showing the signal vectors input into PA1 and PA2 in the case of pure outphasing with constant supply (top right) and outphasing combined with supply modulation (bottom right). The latter shows that a much smaller total outphasing angle is required when supply modulation is included.

outphasing angle and the small output power range of high-efficiency amplification. This can be improved with the addition of supply modulation because the two signal vectors (as shown in Figure 16) can be varied in length as well, thus reducing the need for quickly varying the phase over a large angle. This has been demonstrated using multiple discrete voltage levels supplied to the output stage transistors. Because both a Chireix and LINC transmitter have at least two amplifiers, the supply voltages can be varied in the same way or can be varied between the two amplifiers.

To test the supply-modulated properties of various types of outphasing PAs, a single-stage PA was designed in the 150-nm

GaN process and tested with various output combiners in hybrid Chireix (nonisolated) and LINC (isolated) architectures [42] (Figure 17). The PA with optimized harmonic terminations demonstrated PAE = 70% with 4-W output power at 10 GHz. This architecture demonstrated the performance summarized in Table 3 for a constant-supply voltage, where ΔP_{out} is the output power range when the total efficiency remains within ten points of its peak value and the dynamic P_{out} range is the difference between the maximum and minimum measured output powers. System performance is described by total efficiency.

Discrete supply modulation can improve the back-off efficiency of LINC PAs. In multilevel LINC (ML-LINC), the supplies are varied symmetrically, which reduces power wasted in the isolated combiner. In

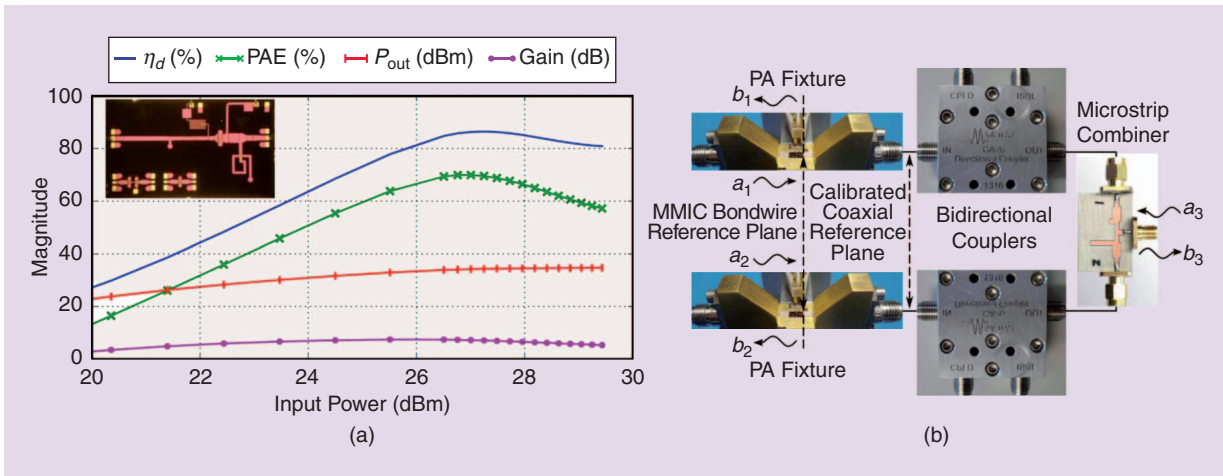


Figure 17. (a) The measured performance of a mounted MMIC PA, showing a peak PAE of 70% at 2.7 W of output power; the inset is a photo of the internal MMIC PA (3.8 mm × 2.3 mm), which is a single-stage design using a 10 × 100-μm pHEMT in Qorvo’s (TriQuint) 150-nm GaN process. (b) A detailed view of the PA-combiner assembly. Several microstrip combiners are designed to provide the desired load modulation.

TABLE 3. A comparison of LINC and Chireix architectures with a constant-supply voltage for a range of outphasing angles, when $\eta_{tot} = P_{out}/(P_{DC}+P_{in})$.

Architecture	Peak P_{out} (dBm)	Peak η_{tot} (%)	ΔP_{out} (dB)	Dynamic P_{out} Range (dB)
LINC	35.8	47.6	0.95	28.9
Chireix	35.7	47.0	1.9	32.1

asymmetric multilevel outphasing (AMO), the supplies are varied independently to achieve further efficiency improvement. Chireix outphasing also benefits from discrete supply modulation, as demonstrated by the multilevel Chireix outphasing (ML-CO) architecture. In Chireix outphasing, the amplitude modulation of the input signal is converted to additional differential phase modulation, which controls the load modulation at the output, thereby controlling the output amplitude. The combiner is designed to modulate the load in a high-efficiency region to maintain efficiency at low output powers. Discrete supply modulation provides an added benefit of reduced dc power consumption by the internal PAs. A measured comparison of different supply modulations is shown in Figure 18, including the ML-LINC, AMO, and ML-CO [42].

Similar performance improvement can be achieved in an integrated MMIC Chireix PA, with measured performance as shown in Figure 19. It turns out that not many discrete voltage levels are needed to achieve efficiency enhancement, and there is no significant improvement above five levels [43].

Conclusions

This article has discussed efficiency improvements when supply modulation is used in conjunction with a high-efficiency PA. It should be noted that ET outperforms

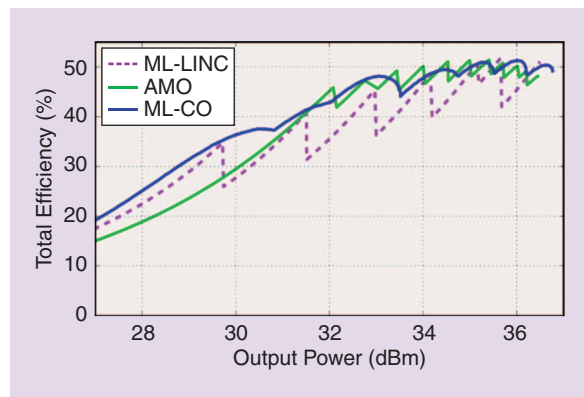


Figure 18. A comparison of ML-LINC, AMO, and ML-CO for two MMIC PAs (Figure 8) with different output combiners and up to seven discrete voltages (from a static measurement).

other architectures if the output power has to change over a large range; for example, if the base station average power varies by 10 dB from daytime to nighttime, the power variation is out of the range that a Doherty can comfortably operate over, but it could be accommodated with an ET amplifier. The Doherty PA also has bandwidth limitations, while variations of ET that do not track the exact envelope, but a reduced bandwidth version, can still have a substantial benefit in efficiency.

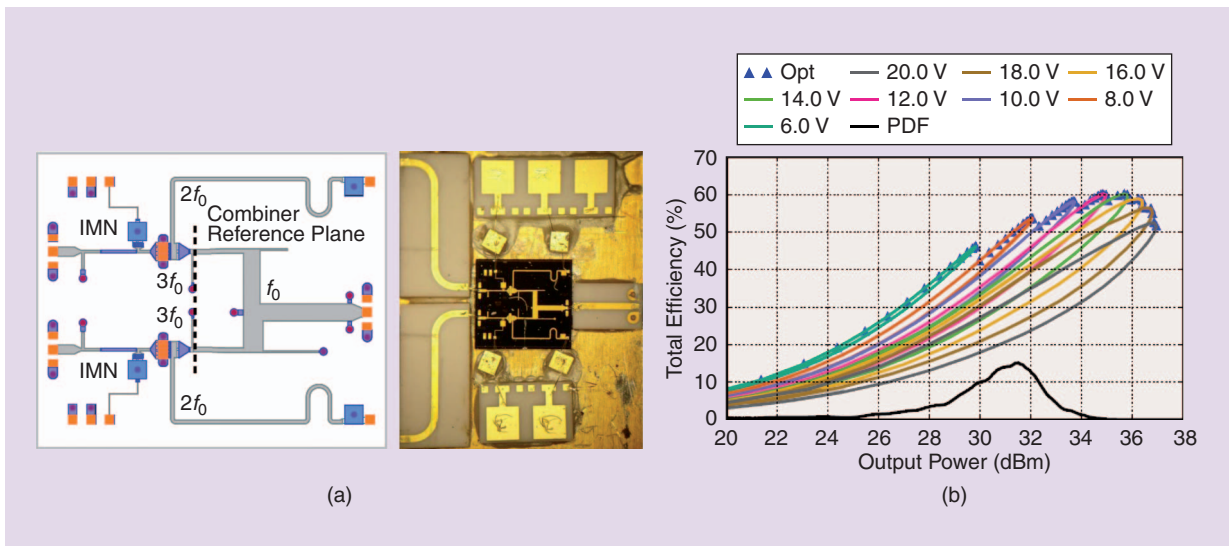


Figure 19. (a) A Chireix outphasing GaN MMIC PA, $3.8 \text{ mm} \times 3.2 \text{ mm}$, and an MMIC mounted in fixture. This MMIC is designed to be modulated with a multilevel supply. (b) The measured phase sweeps for supply levels from 6–20 V in 2-V increments at 9.7 GHz. The optimal trajectory is selected to maximize the total efficiency. In black is the PDF of a 6-dB PAR quadrature phase-shift keying signal which can be used to calculate an average total efficiency of 48% for five and more supply levels [43]. IMN: input matching network.

Supply modulation is not limited to the output-stage drain of a multistage PA. For example, it can be shown that efficiency improves if the drain supplies of both the driver and final stage PA are simultaneously modulated. The addition of gate-supply modulation has been discussed both in the context of Doherty PAs and for improving the linearity of ET PAs. Finally, another type of PA, referred to as harmonically-injected, where one of the PAs in Figure 2 is in class-A mode while the other PA is at the second harmonic, has been demonstrated to give high efficiency over a range of output powers when assisted by supply modulation [44]. The interesting quality of harmonically injected PAs is that they can be efficient and linear, at the expense of the addition of a low-power harmonic injection circuit.

Acknowledgments

I would like to thank all my graduate students and post docs for the hard work and dedication that led to the results shown in this article: Dr. David Sardin, Dr. Scott Schafer, Dr. Michael Litchfield, Dr. Andrew Zai, Michael Coffey, Maxwell Duffy, Dr. Gregor Lasser, Dr. Tibault Reveyrand, Dr. Michael Roberg (now at Qorvo), and Dr. Asmita Dani (now at Infineon), as well as Dr. Chuck Campbell at Qorvo and Prof. Dragan Maksimovic and his students in the Colorado Power Electronics Center. We are grateful for support from the U.S. Office of Naval Research under the Defense Advanced Research Projects Agency's Micro-Power Conversion program and to Dr. Dan Greene and Dr. Paul Maki for support and technical advice, as well as the support of Boeing and Lockheed Martin.

References

- [1] P. Asbeck and Z. Popovic, "ET comes of age: Envelope tracking for higher-efficiency power amplifiers," *IEEE Microwave Mag.*, vol. 17, no. 3, pp. 16–25, Mar. 2016.
- [2] F. Raab, B. E. Sigmon, R. G. Myers, and R. M. Jackson, "L-band transmitter using Kahn EER technique," *IEEE Trans. Microwave Theory Tech.*, vol. 46, pp. 2220–2225, Dec. 1998.
- [3] G. Hanington, P.-F. Chen, P. M. Asbeck, and L. E. Larson, "High-efficiency power amplifier using dynamic power-supply voltage for CDMA applications," *IEEE Trans. Microwave Theory Tech.*, vol. 47, pp. 1471–1476, Aug. 1999.
- [4] M. Ranjan, K. H. Koo, G. Hanington, C. Fallesen, and P. Asbeck, "Microwave power amplifiers with digitally-controlled power supply voltage for high efficiency and linearity," in *Proc. IEEE MTT-S Int. Microwave Symp. Dig.*, 2000, pp. 493–496.
- [5] J. Staudlinger, B. Gilsdorf, D. Newman, G. Sadowiczak, R. Sherman, and T. Quach, "High efficiency CDMA RF power amplifier using dynamic envelope tracking technique," in *Proc. IEEE MTT-S Int. Microwave Symp. Dig.*, 2000, vol. 2, pp. 873–876.
- [6] M. Weiss, F. Raab, and Z. Popovic, "Linearity of X-band class-F PAs in high-efficiency transmitters," *IEEE Trans. Microwave Theory Tech.*, vol. 52, no. 3, pp. 1174–1179, Mar. 2001.
- [7] N. Wang, V. Yousefzadeh, D. Maksimovic, S. Pajic, and Z. B. Popovic, "60% efficient 10-GHz power amplifier with dynamic drain bias control," *IEEE Trans. Microwave Theory Tech.*, pp. 1077–1081, 2004.
- [8] F. Wang, A. Ojo, D. Kimball, P. Asbeck, and L. Larson, "Envelope tracking power amplifier with pre-distortion linearization for WLAN 802.11g," in *Proc. IEEE MTT-S Int. Microwave Symp. Dig.*, 2004, vol. 3, pp. 1543–1546.
- [9] D. Kimball, J. Jeong, C. Hsia, P. Draxler, S. Lanfranco, W. Nagy, K. Linthicum, L. E. Larson, and P. M. Asbeck, "High-efficiency envelope-tracking W-CDMA base-station amplifier using GaN HFETs," *IEEE Trans. Microwave Theory Tech.*, pp. 3848–3856, Nov. 2006.
- [10] H. Nemat, C. Fager, U. Gustavsson, R. Jos, and H. Zirath, "Characterization of switched mode LDMOS and GaN power amplifiers for optimal use in polar transmitter architectures," in *Proc. IEEE MTT-S Int. Microwave Symp. Dig.*, 2008, pp. 1505–1508.

- [11] N. Lopez, et al., "A high-efficiency linear polar transmitter for EDGE," *IEEE Radio Wireless Week*, 2008, pp. 199–202.
- [12] M. Pelk, W. C. E. Neo, J. R. Gajadharsing, R. S. Pengelly, and L. C. N. de Vreede, "A high-efficiency 100-W GaN three-way doherty amplifier for base-station applications," *IEEE Trans. Microwave Theory Tech.*, vol. 56, no. 7, pp. 1582–1591, June 2008.
- [13] C. J. Li, C. T. Chen, T. S. Horng, J. K. Jau, and J. Y. Li, "High average-efficiency multimode rf transmitter using a hybrid quadrature polar modulator," *IEEE Trans. Circuits Syst.*, vol. 55, no. 3, pp. 249–253, 2008.
- [14] I. Kim, J. Kim, J. Moon, and B. Kim, "Optimized envelope shaping for hybrid EER transmitter of mobile WiMAX—Optimized ET operation," *IEEE Microwave Wireless Commun.*, vol. 19, no. 5, pp. 335–337, 2009.
- [15] J. Qureshi et al., "A 90-W peak power GaN outphasing amplifier with optimum input signal conditioning," *IEEE Trans. Microwave Theory Tech.*, vol. 57, no. 8, pp. 1925–1935, Aug. 2009.
- [16] J. Jeong et al., "High-efficiency WCDMA envelope tracking base-station amplifier implemented with GaAs HVHBTs," *IEEE J. Solid-State Circuits*, vol. 44, no. 10, pp. 2629–2639, 2009.
- [17] J. Moon, et al., "Doherty amplifier with envelope tracking for high efficiency," in *Proc. IEEE MTT-S Int. Microwave Symp. Dig.*, Anaheim, CA, 2010, pp. 1–1.
- [18] C. Hsia et al., "Digitally assisted dual-switch high-efficiency envelope amplifier for envelope-tracking base-station power amplifiers," *IEEE Trans. Microwave Theory Tech.*, vol. 60, no. 6, pp. 2943–2952, Nov. 2011.
- [19] M. Mercanti, A. Cidronali, S. Maurri, and G. Manes, "HEMT GaAs/GaN power amplifiers architecture with discrete dynamic voltage bias control in envelope tracking RF transmitter for W-CDMA signals," in *Proc. IEEE Topical Conf. Power Amplifiers for Wireless and Radio Applications*, 2011, pp. 9–12.
- [20] M. van der Heijden, M. Acar, J. S. Vromans, and D. A. Calvillo-Cortes, "A 19W high-efficiency wide-band CMOS-GaN class-E Chireix RF outphasing power amplifier," in *Proc. IEEE MTT-S Int. Microwave Symp. Dig.*, 2011, pp. 1–4.
- [21] J. Hoversten, S. Schafer, M. Roberg, M. Norris, D. Maksimovic, and Z. Popovic, "Co-design of PA, supply, and signal processing for linear supply-modulated RF transmitters," *IEEE Trans. Microwave Theory Tech.*, vol. 60, no. 6, pp. 2010–2020, June 2012.
- [22] C. Yu and A. Zhu, "A single envelope modulator-based envelope-tracking structure for multiple-input and multiple-output wireless transmitters," *IEEE Trans. Microwave Theory Tech.*, pp. 3317–3327, 2012.
- [23] D. Calvillo-Cortes, M. P. van der Heijden, and L. C. N. de Vreede, "A 70W package-integrated Class-E Chireix outphasing RF power amplifier," in *Proc. IEEE MTT-S Int. Microwave Symp. Dig.*, 2013, pp. 1–3.
- [24] S. Schafer, M. Litchfield, A. Zai, Z. Popović, and C. Campbell, "X-Band MMIC GaN power amplifiers designed for high-efficiency supply-modulated transmitters," in *Proc. IEEE MTT-S Int. Microwave Symp. Dig.*, pp. 1–3, 2013.
- [25] A. Zai, D. Li, S. Schafer and Z. Popovic, "High-efficiency X-Band MMIC GaN Power amplifiers with supply modulation," in *Proc. IEEE MTT-S Int. Microwave Symp. Dig.*, 2014, pp. 1–4.
- [26] E. McCune, *Dynamic Power Supply Transmitters: Envelope Tracking, Direct Polar, and Hybrid Combinations*. Cambridge, U.K.: Cambridge Univ. Press, 2015.
- [27] D. F. Kimball, H. Kazeimi, J. J. Yan, P. T. Theilmann, I. Telleiz, and G. Collins, "Envelope modulator X-Band MMICs on highly integrated 3D tunable microcoax substrate," in *Proc. IEEE Compound Semiconductor Integrated Circuit Symp.*, New Orleans, LA, 2015, pp. 1–4.
- [28] Y. Zhang, M. Rodríguez, and D. Maksimovic, "High-frequency integrated gate drivers for half-bridge GaN power stage," in *Proc. IEEE COMPEL*, June 2014.
- [29] S. Schafer and Z. Popović, "Multi-frequency measurements for supply modulated transmitters," in *IEEE Trans. Microwave Theory Tech.*, vol. 63, no. 9, pp. 2931–2941, Sept. 2015.
- [30] Available: <http://cp.literature.agilent.com/litweb/pdf/rfde2006/pdf/rfdecktsimenv.pdf>
- [31] J. Jeong, D. F. Kimball, M. Kwak, C. Hsia, P. Draxler, and P. M. Asbeck, "Wideband envelope tracking power amplifiers with reduced bandwidth power supply waveforms and adaptive digital predistortion techniques," *IEEE Trans. Microwave Theory Tech.*, vol. 57, no. 12, pp. 3307, Dec. 2009.
- [32] G. Montoro, P. Gilabert, J. Berenguer, and E. Bertran, "Digital predistortion of envelope tracking amplifiers driven by slew-rate limited envelopes," in *Proc. IEEE MTT-S Int. Microwave Symp. Dig.*, 2011, pp. 1–1.
- [33] Y. Zhang, M. Rodríguez, and D. Maksimović, "Very high frequency PWM buck converters using monolithic GaN half-bridge power stages with integrated gate drivers," *IEEE Trans. Power Electron.*, vol. 31, no. 11, pp. 7926–7942, Nov. 2016.
- [34] A. Sepahvand, Y. Zhang, and D. Maksimovic, "High efficiency 20-400 MHz PWM converters using air-core inductors and monolithic power stages in a normally-off GaN process," in *Proc. IEEE Applied Power Electronics Conf.*, 2016, pp. 580–586.
- [35] A. Sepahvand, et al., "Monolithic multilevel GaN converter for envelope tracking in RF power amplifiers," in *Proc. IEEE Energy Conversion Congress and Exposition Conf.*, 2016, pp. 1–7.
- [36] C. Florian, et al., "Efficient programmable pulse shaping for X-Band GaN MMIC radar power amplifiers," *IEEE Trans. Microwave Theory Tech.*, no. 99, pp. 1–11.
- [37] C. Florian, T. Cappello, R. P. Paganelli, D. Niessen, and F. Filicori, "Envelope tracking of an RF high power amplifier with an 8-level digitally controlled GaN-on-Si supply modulator," *IEEE Trans. Microwave Theory Tech.*, vol. 63, no. 8, pp. 2589–2602, Aug. 2015.
- [38] M. Litchfield, T. Cappello, C. Florian, and Z. Popovic, "X-band multi-level chireix outphasing PA with a GaN Discrete supply modulator MMIC," in *Proc. IEEE Compound Semic. Int. Circuit Symp.*, Austin, TX, 2016.
- [39] D. Sardin, et al., "High efficiency 15-500MHz wideband cascode GaN HEMT MMIC amplifiers," in *Proc. IEEE MTT-S Int. Microwave Symp. Dig.*, Tampa, FL, 2014, pp. 1–4.
- [40] Y. Zhang, M. Rodríguez, and D. Maksimović, "Output filter design in high-efficiency wide-bandwidth multi-phase buck envelope amplifiers," in *Proc. IEEE Applied Power Electronics Conf. and Exposition*, Charlotte, NC, 2015, pp. 2026–2032.
- [41] M. Coffey, P. MomenRoodaki, A. Zai, and Z. Popovic, "A 4.2-W 10-GHz GaN MMIC doherty power amplifier," in *Proc. IEEE Compound Semiconductor Integrated Circuit Symp.*, New Orleans, LA, 2015, pp. 1–4.
- [42] M. Litchfield, T. Reveyrand, and Z. Popović, "Load modulation measurements of X-Band outphasing power amplifiers," *IEEE Trans. Microw. Theory Tech.*, vol. 63, no. 12, pp. 4119–4129, Dec. 2015.
- [43] M. Litchfield and Z. Popovic, "Multi-level Chireix outphasing GaN MMIC PA," in *Proc. IEEE Compound Semiconductor Integrated Circuit Symp.*, New Orleans, LA, 2015, pp. 1–4.
- [44] A. Dani, M. Coffey, and Z. Popović, "Efficient linear supply-modulated PA with harmonic injection," in *Proc. European Microwave Conf.*, Nuremberg, 2013, pp. 541–544.

